Inclination and rolling motion effect on subcooled flow boiling pressure drop through annulus channel with helical finned heater

Hyukjae Ko, Chang Won Lee, Jin-Seong Yoo, Heepyo Hong, Ja Hyun Ku, Goon-Cherl Park, Hyoung Kyu Cho*
Dept. of nuclear engineering, Seoul National Univ., 1 Gwanak-ro, Gwanak-gu, Seoul 08826
**Corresponding author: chohk@snu.ac.kr*

1. Introduction

Unlike land-based reactors, off-shore reactors are directly exposed to the oscillatory nature of the ocean. With growing demand of safety assurance for nuclear reactors, assessment of additional force effect on thermal-hydraulic behavior in the reactor systems is critical for those floating reactors. As part of an effort to advance understanding of the effect, various thermal-hydraulic experimental and analytic studies considering motion conditions have been conducted [1, 2]. At Seoul national university, rolling and heaving motion effect on CHF (critical heat flux) is being studied with NEOUL-R and NEOUL-H platform. By utilizing those platforms, motion effect on pressure drop and heat transfer characteristics are also investigated with expectations for contributing the floating reactor design and safety analysis capability enhancement.

In this study, subcooled flow boiling pressure drop was measured under inclined and rolling conditions with the NEOUL-R platform. Additional force effect on pressure drop were assessed, corresponding to each condition.

2. Experimental facility and procedure

2.1 Experimental facility

The experimental facility consists of NEOUL-R platform and a test loop. The facility was established to explore CHF phenomenon and thermal-hydraulic characteristics of subcooled flow boiling under static inclination and rolling motion conditions. The platform can maintain inclined condition up to 45° from vertical position and rolling motion condition with minimum period of 6 seconds.

The test loop is composed of a pump, a pre-heater, a throttling valve, a test section, and two heat exchangers (condenser and cooler). As measurement instruments, there are two pressure transmitters, a differential pressure transmitter, a Coriolis flowmeter, multiple thermocouples, etc. [3]. The locations of the pressure and differential pressure measurements were shown in Fig. 1.

The test section was designed to simulate the coolant flow around the heater rod with a working fluid, R-134a. A spirally finned heater rod having geometry of four fins wound around a bare rod was used, which was previously studied for CHF phenomenon characteristics [4].

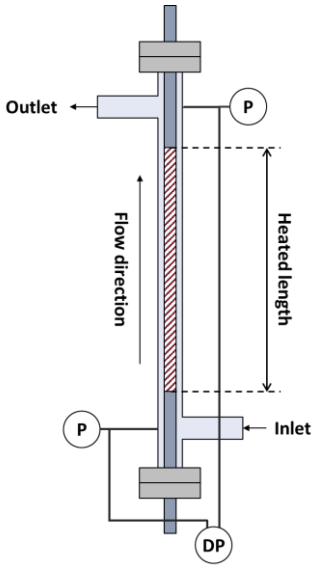

Fig. 1. Schematics of test section and pressure measurement devices

2.2 Experiment and data reduction procedure

The experiments were conducted for each vertical, inclined, and rolling conditions by increasing power stepwise from zero to near CHF while maintaining thermal-hydraulic conditions: outlet pressure, inlet temperature, and mass flux.

As shown in Eq. (1) measurement of differential pressure transmitter consist of pressure drop through the test section and static pressure drop in impulse lines. In Eq. (1), ΔP_{DP} , ΔP_{TS} , and ΔP_{Imp} denote measured pressure drop, pressure drop in the test section, and pressure drop in impulse lines. To examine pressure drops through the test section, pressure drops in impulse lines were calculated and compensated to measured pressure drops with Eq. (2), assuming static liquid filled in impulse lines. In Eq. (2), ρ_{liq}, $\vec{a}$, $\Sigma\vec{h}_{Imp}$ each indicates liquid density filled in impulse lines, exerted acceleration, and sum of each impulse line segment vectors.

The acceleration is calculated with Eq. (3), where $\vec{g}$ and $\vec{a}_{cen}(\theta)$ denoting gravitational acceleration vector and centrifugal acceleration vector which is a function of instantaneous angle, respectively. Considering rolling motion simulated by platform follows ideal sinusoidal wave function, centrifugal acceleration can be derived as Eq. (4). Variables in Eq. (4) are θ_{Max}, T, h_{TS}, and $\vec{r}$. First two variables indicate max angle and period of rolling, third one is height of the test section, and the last one is axial position vector originating from axis of rolling motion.

$$\Delta P_{DP} = \Delta P_{TS} - \Delta P_{Imp} \quad (1)$$

$$\Delta P_{Imp} = \rho_{liq}\vec{a} \cdot \left(\Sigma \vec{h}_{Imp}\right) \quad (2)$$

$$a = \vec{g} + \vec{a}_{cen}(\theta) \quad (3)$$

$$\vec{a}_{cen}(\theta) = \frac{1}{h_{TS}} \int_{TS} \theta_{Max}^2 \left(\frac{2\pi}{T}\right)^2 \left(1 - \left(\frac{\theta}{\theta_{Max}}\right)^2\right) \vec{r} d\vec{r} \quad (4)$$

3. Results and analysis

3.1 Analysis method

The static pressure drop of fluid in the test section varies proportionally to the density and acceleration. Thus, under this experiment condition, static pressure drop is expected to decrease with mass quality increment and linearly vary with additional force. On the other hand, dynamic pressure drop through the test section tends to increase with exit quality under subcooled flow boiling condition [5]. However, relationship with dynamic pressure drop and additional force is uncertain, especially under subcooled flow boiling condition. Therefore, key part of this study is evaluation of additional force effect on dynamic pressure drop, driven by inclination and rolling motion and its contribution to total pressure drop.

To assess dynamic and static pressure drop separately, total pressure drop decomposition method was established utilizing existing models. Considering static pressure drop can be calculated with density and acceleration, estimation of axial density profile under subcooled flow boiling condition is required.

Based on the uniform axial power distribution of the heater, enthalpy of fluid is assumed to increase linearly. Therefore, axial location where flow quality becomes non-zero, and quality at the EHL (End of Heated Length), average density in the test section can be estimated, assuming homogeneous flow. The non-zero quality location is determined with the OSV (Onset of Significant void) point, defined as vapor starts existing in bulk region of the flow. The OSV point was calculated by comparing flow enthalpy and predicted OSV enthalpy utilizing Saha and Zuber's model [6]. For mass quality at EHL, Ahmad's model [7] was utilized, which predicts mass quality from thermal equilibrium quality and OSV enthalpy.

3.2 Static vertical results

At first, vertical stationary experiment results with 6 different thermal-hydraulic conditions were shown in Fig. 2 There are two notable trends in the figure: one is that total pressure drops increase with mass flux and the other is that total pressure drops decrease with quality. The former is a common phenomenon, as the frictional pressure drop increases with flow speed, the latter can be explained by static pressure drop decrease with density. One more thing to note is that the negative gradient of the total pressure drop with respect to quality reduces with mass flux increase, which can be assessed as the result of dynamic pressure drop fraction enlargement.

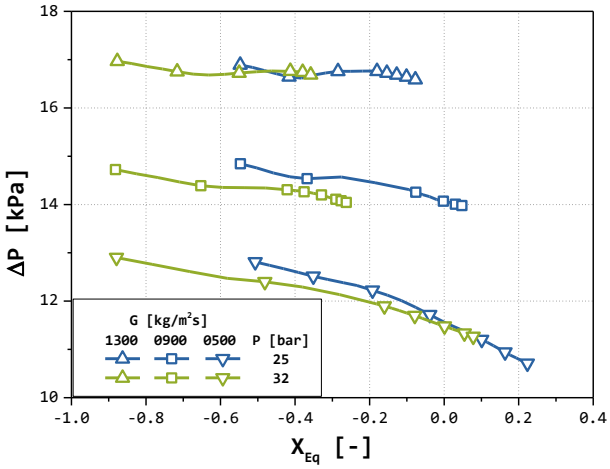

Fig. 2. Vertical conditon total pressure drop vs. thermal equilibrium exit quality results

Fig. 3 shows the decomposition results under 3 different thermal-hydraulic conditions. Case (a) was selected as the reference case and Case (b) has higher mass flux, and Case (c) has higher pressure than it.

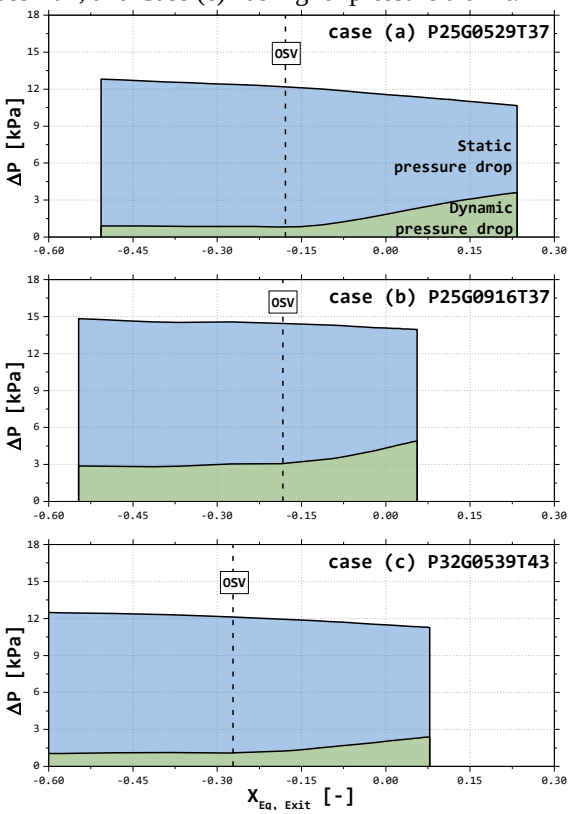

Fig. 3. Vertical condition total pressure drop decomposition results. [case (a) P = 25 bar, G = 529 kg/m^{2}s, T_{sub}=37 K (b) P = 25 bar G = 916 kg/m^{2}s T_{sub}=37 K (c) P = 32 bar G = 539 kg/m^{2}s T_{sub} = 43 K]

Commonly, the dynamic pressure drop gradient increased significantly after initiation of OSV. When the

mass flux gets large, it is apparent that dynamic pressure drop fraction increase, compensating static pressure drop decrement trend. For higher pressure case, both static and dynamic pressure drop trend declined, due to density difference between phases decreased.

3.3 Inclination effect on pressure drop

In this section, inclination effect on pressure drop was assessed for the reference thermal-hydraulic condition.

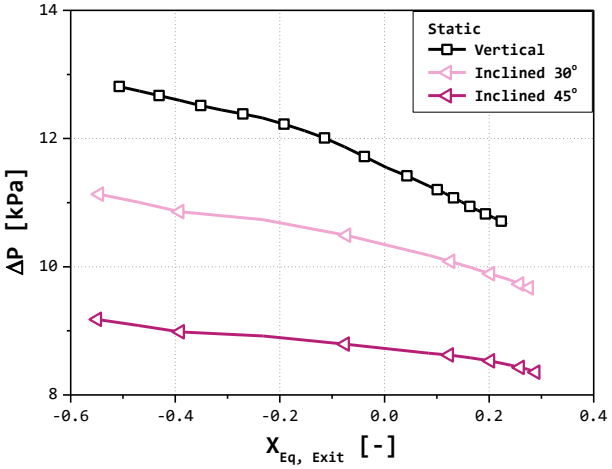

Fig. 4. Total pressure drop vs. $X_{Eq, Exit}$ under vertical and inclination condition results

As shown in Fig. 4, the total pressure drop decrease with inclination angle. Also, in high-quality region, total pressure drop gradient increased with inclination angle. Considering effective gravitational acceleration is proportional to cosine of inclination angle, static pressure drop leading the overall trend can be expected.

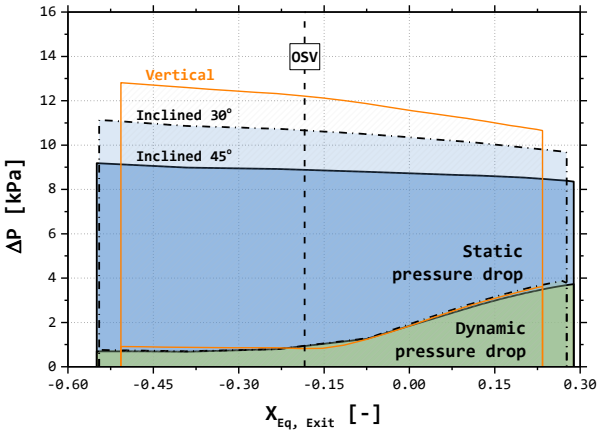

Fig. 5. Total pressure drop for vertical, inclined 30°, and 45° case decomposition results

Decomposition of total pressure drop results for inclined conditions shown in Fig. 5. Reduction of the static pressure drop portion with inclination angle is apparent in figure. Contrarily, the inclination effect on dynamic pressure drop seems to be negligible.

3.4 Rolling effect on pressure drop

In the case of the rolling condition, the additional force affecting pressure drop to vary with time. Therefore, the time-averaged total pressure drop results are presented forehand and afterward, the maximum and minimum total pressure drop for each power step are discussed.

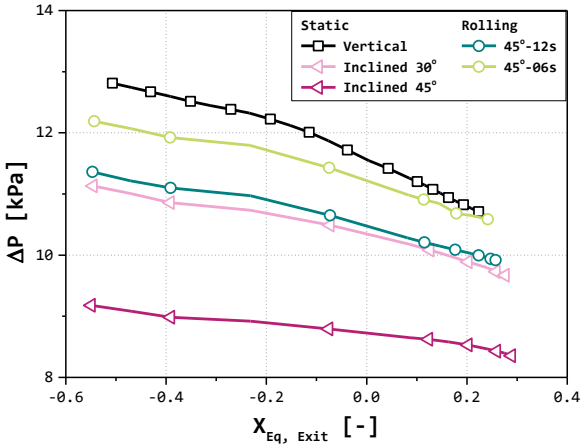

Fig. 6. Total pressure drop vs. $X_{Eq, Exit}$ of vertical, inclined, and averaged rolling condition results

In Fig. 6, the averaged total pressure drop results from 2 rolling period conditions were plotted with the static vertical and inclined conditions results. The major difference between rolling conditions compared to static results is that centrifugal acceleration and gravitational acceleration affects the static pressure drop simultaneously. If centrifugal force can be neglected, the pressured drop with the rolling motion of 45° would converge to the result under the static inclination with 30°, because the time-averaged angle of the rolling motion is 28.6°. As can be seen in Fig. 6, the averaged pressure drop of rolling 45° and 12 seconds period result lays closer to the 30° inclination pressure drop result than shorter period result. Therefore, increase of deviation between pressure drop results under rolling conditions with respect to the period is a clear evident of centrifugal force affecting pressure drop.

The maximum and minimum total pressure drop results of 45° rolling with 6 and 12 s period condition are plotted in Fig. 7. Considering centrifugal acceleration reaches its maximum when passing vertical position, difference between stationary vertical and rolling condition max results clearly represents effect of centrifugal force. In opposition, small difference with the minimum results and inclined 45° results can be explained as when test section reaches edge of rolling motion range, centrifugal acceleration is equal to zero becoming equivalent condition as stationary inclined state.

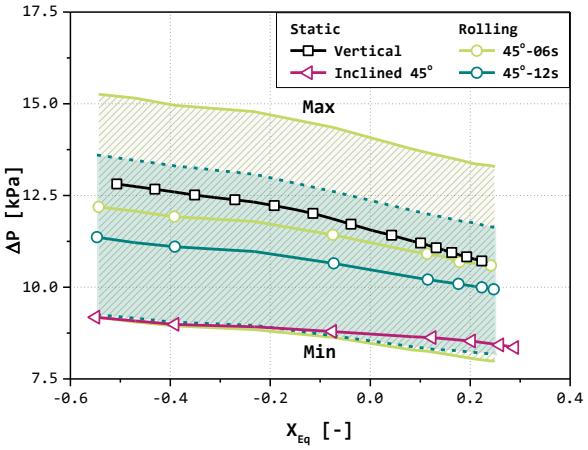

Fig. 7. Average, maximum, and minimum total pressure drop under rolling conditions plotted with static vertical and inclined 45° results

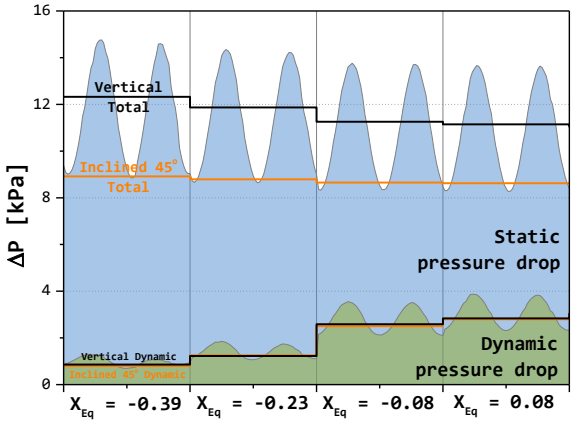

Fig. 8. Four cases of X_{Eq} near OSV point total pressure drop under 45° & 6s rolling condition decomposition results

At Fig. 8, single period (-45° → 45° → -45°), instantaneous results were extracted and decomposed for four power steps: 2 from pre-OSV points and 2 for post-OSV points and compared with stationary vertical and inclined condition results for corresponding thermal equilibrium quality. The total pressure drop result reaches its maximum value when the test section passing vertical position and minimum value at inclined 45° position with major contribution of the static pressure drop can be seen in the figure. For post-OSV results, the static pressure drop still dominates the total pressure drop with some minor fluctuation increase of dynamic pressure drop. Therefore, even under the rolling condition static pressure drop leads the total pressure drop difference and deviation of dynamic pressure drop increased at post-OSV conditions, however contribution to total pressure drop seems negligible.

4. Conclusions

Effect of inclination and rolling conditions on pressure drop were investigated experimentally. For assessment of the results, measured total pressure drop was assessed first, and then decomposed to static and dynamic pressure drops for evaluation of the effect separately. Overall results showed total pressure drop deviates with exerted additional force, primarily driven by static pressure drop difference corresponding to additional force variation. On the other hand, dynamic pressure drop showed relatively minor deviation with additional force implying that the effect of additional force on dynamic pressure drop can be assumed negligible.

Vertical condition

Total pressure drop increased with mass flux, due to dynamic pressure drop increase. The decreasing trend of total pressure drop with quality was compensated with respect to the mass flux increment.

Inclined condition

Inclination angle increment reduced total pressure drop significantly. After decomposition, it was apparent that the reduction was driven by the static pressure drop.

Rolling condition

The maximum total pressure drop increased with shorter period, clearly showing effect of centrifugal acceleration. Like inclined condition results, static pressure drop affected by additional force significantly, driving the total result. On the contrary, additional force effect on the dynamic pressure drop seemed negligible.

REFERENCES

[1] J.S. Hwang et al., Characteristics of critical heat flux under rolling condition for flow boiling in a vertical tube, Nuclear Engineering and Design, 252, 153–162, 2012.
[2] T. Otsuji and A. Kurosawa, Critical heat flux of forced convection boiling in an oscillating acceleration field—III. Reduction mechanism of CHF in subcooled flow boiling, Nuclear Engineering and Design, 79(1), 19-30, 1984.
[3] G. W. Kim, Experimental investigation of critical heat flux on a single heater rod under inclined and rolling conditions, Ph.D. thesis, Seoul National University, 2021.
[4] C. W. Lee et al., "Experimental investigation of CHF on helical finned heater under the static inclination and rolling conditions", Transactions of the Korean Nuclear Society Spring Meeting, Jeju, Korea, May 19-20, 2022
[5] Sung-Min Kim and Issam Mudawar, "Review of databases and predictive methods for pressure drop in adiabatic, condensing and boiling mini/micro-channel flows", International Journal of Heat and Mass Transfer,Vol. 77, 2014, pp 74-97,
[6] Saha P., and Zuber, "Point of net vapor generation and vapor void fraction in subcooled boiling", Proceedings of Fifth International Heat Transfer Conference, Vol. 4, pp. 175-179.
[7] S. Y. Ahmad, "Axial Distribution of Bulk Temperature and Void Fraction in a Heated Channel With Inlet Subcooling", ASME J. Heat Transfer 92(1970) pp.595-609.